Electron and photon diagnostics for plasma acceleration-based FELs

Marie Labat,* Moussa El Ajjouri, Nicolas Hubert, Thomas Andre, Alexandre Loulergue and Marie-Emmanuelle Couprie

Synchrotron SOLEIL, Saint-Aubin, 91191 Gif-sur-Yvette, France.
*Correspondence e-mail: marie.labat@synchrotron-soleil.fr

It is now well established that laser plasma acceleration (LPA) is an innovative and good candidate in the beam acceleration field. Relativistic beams are indeed produced up to several GeV but their quality remains to be demonstrated in the highly demanding case of free-electron lasers (FELs). Several experiments have already shown the feasibility of synchrotron radiation delivery based on LPA but free-electron lasing has still to be achieved. Since the quality of the LPA beam inside the undulator is the critical issue, any LPA-based FEL experiment requires a refined characterization of the beam properties along the transport line and of the photon beam at the undulator exit. This characterization relies on diagnostics which must be adapted to the LPA specificities. Here, the electron and photon diagnostics already used on LPAs and required for LPA-based FELs are reviewed, and the critical points are illustrated using recent experiments performed around the world.

1. Introduction

Free-electron lasers (FELs) (Madey, 1971) are presently the most brilliant light sources and precious tools for time-resolved studies of molecular and atomic dynamics (Zewail, 2003). Several facilities are routinely in operation for users in the hard X-ray range (Emma *et al.*, 2010; Ishikawa *et al.*, 2012) as in the XUV and soft X-ray range (Ackermann *et al.*, 2007; Allaria *et al.*, 2013). A FEL is a system consisting of a relativistic electron beam and an undulator, which enables the spontaneous synchrotron radiation created by the particles oscillating in the undulator to be amplified, or an external seed injected together with the electron beam in the undulator. This amplification is exponential in $\exp(z/L_G)$, z being the longitudinal coordinate along the undulator and L_G the so-called gain length (Dattoli *et al.*, 1993; Kim & Xie, 1993). This gain length is directly related to the electron beam parameters according to $L_G = [\lambda_u/(4\pi\sqrt{3})]\gamma(\sigma_x\sigma_y/\hat{I})^{1/3}$, with λ_u the undulator period, γ the usual Lorentz factor, $\hat{I}$ the peak current and $\sigma_{x,y}$ the transverse beam sizes. A high-gain FEL therefore corresponds to a short gain length system, which requires a high density, *i.e.* high-quality electron beam.

Present FELs are based on radio-frequency accelerators (RFAs) which offer the highest quality electron beams: typically charges of 10 pC up to 1 nC with a normalized emittance between 0.1 and 1π mm mrad and an energy spread which does not exceed the 0.01% level. Thanks to decades of operation and improvements, the stability of those parameters can stay at the percent level during typically days of operation. Nevertheless, their accelerating gradient is limited to 100 MV m^{-1}.

In the late 1970s, a compact and elegant alternative to the RF technology was suggested by Tajima & Dawson (1979) which proposed laser-generated plasma wakes to accelerate particles. Impressive developments (Pittman *et al.*, 2002; Pukhov & Meyer-ter-Vehn, 2002) led in 2004 to the first demonstration of plasma acceleration (Mangles *et al.*, 2004; Geddes *et al.*, 2004; Faure *et al.*, 2004). Laser plasma accelerators (LPAs) were born. Since then, the quality of LPA beams has kept increasing (Chien *et al.*, 2005; Leemans *et al.*, 2006; Faure *et al.*, 2006; Geddes *et al.*, 2008). Still, although the six-dimensional brightness of the LPA beams can now be comparable with that of the RFAs (Schroeder *et al.*, 2012), much more effort is necessary in terms of available charge (few pC), energy spread (above a few %) and divergence (few mrad) for FEL applications. On the other hand, LPAs can deliver above 100 GV m^{-1} accelerating gradients, which could be one way towards more compact accelerators and, consequently, towards more compact FELs. Together with the novelty of the technology, this motivated several groups to try the operation of an LPA-based FEL.

In 2008, Schlenvoigt *et al.* (2008) observed the first synchrotron radiation (SR) resulting from an LPA beam travelling through an undulator. Using a 60 MeV beam together with a 1 m-long undulator of 20 mm period, they recorded an SR spectrum centered at 740 nm. Four other groups then also successfully produced SR both in the UV and visible range (Fuchs *et al.*, 2009; Lambert *et al.*, 2012; Anania *et al.*, 2014; Couprie *et al.*, 2018). The key features of these

Table 1
LPA-based SR experiments that reported SR observations at an undulator exit.

E_e: electron beam energy in MeV. λ_u: undulator period in mm. L_u: undulator length in m. λ_r: resonance wavelength in nm. Transp: transport magnetic elements. Q-lenses: magnetic lenses. EMQ: electromagnetic quadrupole. PMQ: permanent-magnet quadrupole.

Experiment Country	IOQ Jena Germany	MPQI Germany	LOA France	University of Strathclyde UK	LOA and SOLEIL France
E_e	60	200	100–150	100	176
λ_u	20	5	18.2	15	18
L_u	1	0.3	0.6	0.5	2
λ_R	740	18	250–400	220	200
Transp.	–	2 Q-lenses	3 EMQs	3 PMQ + 3 EMQs	3 PMQ + 4 dipoles + 4 EMQs

experiments are summarized in Table 1, and the COXINEL (COherent X-ray source INferred from Electrons accelerated by Laser) most advanced layout is given as an example in Fig. 1. At least two other groups are presently working on the same topic: Leemans *et al.* at Lawrence Berkeley National Laboratory, USA, and Sano *et al.* on the ImPACT project, Japan.

However, none of the experiments which produced SR have succeeded in amplifying this SR. The gain resulting from the large divergence and energy spread of the LPA beam remains too low with respect to the undulator length used.

To deal with these realistic high energy spread and high divergence, three techniques have been proposed: horizontally disperse and couple the beam in a transverse gradient undulator (Huang *et al.*, 2012); decompress and couple the beam in a suitably tapered undulator (Maier *et al.*, 2012; Seggebrock *et al.*, 2013; Couprie *et al.*, 2014); and, finally, decompress and synchronize the beam waist advance with the FEL slippage (Loulergue *et al.*, 2015). While the first two
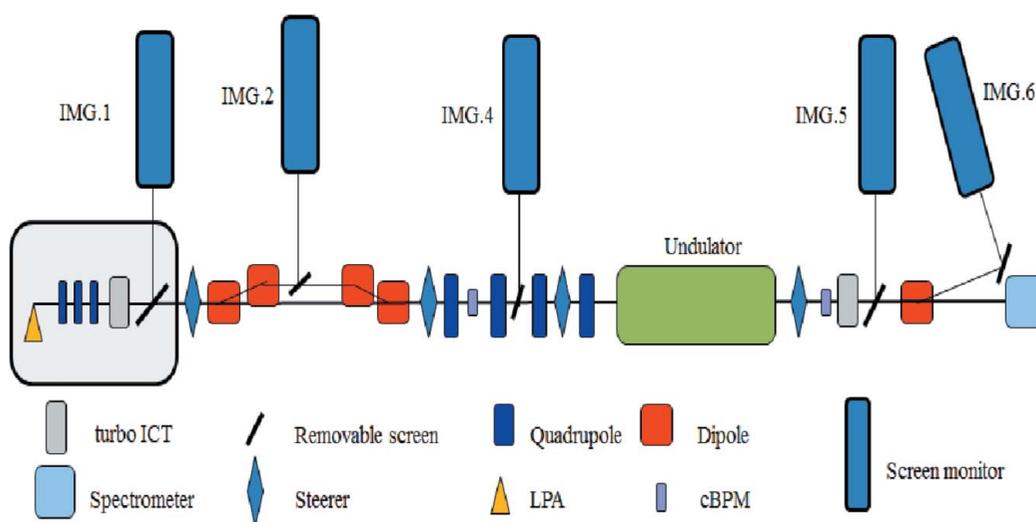

Figure 1
Layout of the COXINEL experiment consisting from left to right of: LPA (IR laser focused into a gas jet); three permanent-magnet quadrupoles (QUAPEVA) to refocus the beam; turbo-ICT; screen monitor (IMG.1); steerer to correct the beam orbit; four dipoles forming a chicane to decompress the beam with a screen monitor (IMG.2) in its middle; a second steerer; four electromagnetic quadrupoles to match the beam in the undulator, in between the first and second a cavity beam position monitor (cBPM), in between the second and third a fourth screen monitor (IMG.4) and in between the third and fourth a third steerer; undulator of 110 periods of 18 mm; a fourth steerer; final cBPM; a last turbo-ICT; screen monitor (IMG.5); dump dipole; final screen monitor (IMG.6); and a spectrometer in the visible range.

methods have never been implemented, the last one, referred to as chromatic matching, is presently being tested on COXINEL (Couprie *et al.*, 2016).

Whatever the final configuration, the demonstration and further operation of an LPA-based FEL requires dedicated diagnostics which should be adapted to the LPA's specificities. In this paper, we review the main diagnostics operated on LPAs for electron beam characterization and manipulation in transport lines, addressing main issues and recent achievements. We also review the photon diagnostics used up to now in the attempts at LPA-based FEL experiments, underlying the main difficulties related to their implementation on an LPA line.

2. Electron beam diagnostics

2.1. Charge measurements

Charge measurements on RFAs mainly rely on Faraday cups (Brown & Tautfest, 1956), integrating current transformers (ICTs) (Unser *et al.*, 1989) and Rogowski coils (Rogowski & Steinhaus, 1912). But the very strong electromagnetic pulse (EMP) environment of the LPAs tends to spoil any electronic-based measurement. This is why charge measurements on LPAs essentially rely on photoluminescence-based detectors, among which the most popular are imaging plates and Lanex screens.

2.1.1. Imaging plates (IPs). An IP is a multilayer film with a photostimulable phosphor layer. Irradiation by an electron beam excites electron–hole pairs in the sensitive phosphor, which can remain trapped and later detrapped for detection using photostimulated luminescence with a scanner. IPs have been calibrated on RFAs *versus* beam energy up to 100 MeV using Rogowski coils (Tanaka *et al.*, 2005) and *versus* charge up to 120 pC using ICTs (Zeil *et al.*, 2010). Their dynamic range is large ($\sim 10^5$) and they offer a high sensitivity. But before processing the films, one has to wait for the electron–hole pairs' decay to stabilize in time, which typically requires a couple of hours. In spite of this 'fading' effect, which makes them unsuitable for high-repetition-rate measurements, they remain a reference in terms of absolute charge measurement in the community (Tanaka *et al.*, 2005).

2.1.2. Lanex screens. Lanex screens (Gd2O2S:Tb) are scintillators consisting of a mixture of phosphor powder in a urethane binder. When the electron beam passes through the screen, it deposits energy which results in light emission in the visible range. The photon distribution can then simply be imaged by an objective on a charge couple device (CCD) camera. Lanex screens have been calibrated on RFAs up to an energy of 1.5 GeV and for charges up to 800 pC (Nakamura *et al.*, 2011). Since then, they have been extensively used on LPAs to provide absolute charge measurements (Glinec *et al.*, 2006). It is this technique which has been used on all but the COXINEL LPA-based SR experiments to measure bunch charges in the 0.1 to 30 pC range (Schlenvoigt *et al.*, 2008; Fuchs *et al.*, 2009; Lambert *et al.*, 2012; Anania *et al.*, 2014).

2.1.3. ICTs. Whereas IPs and Lanex screens are destructive measurements, ICTs are non-invasive. But, relying on electronics which integrate the charge over a time window of hundreds of microseconds, they are not well adapted to the LPAs' strong EMP environment, low-charge beams and single-shot requirement. Nevertheless, ICTs from Bergoz (http://www.bergoz.com/en) were implemented on LPAs and compared with Lanex screen measurements. In a first work (Glinec *et al.*, 2006), a discrepancy up to a factor of eight, varying shot-to-shot, was reported. But, in a more recent work (Nakamura *et al.*, 2011), a very good agreement was obtained. The (new) reliability of the ICT was attributed by the authors to: (i) the special care taken to avoid EMP effects (cable extension for time separation of signals, cable shielding, arranged route), (ii) the installation of a metallic foil and of a low-acceptance aperture to prevent particle/radiation hit on the ICT, (iii) the installation out of vacuum and on a ceramic gap of the ICT so that electron beams propagate in vacuum with minimum disturbance, and (iv) the large spacing of the ICT and Lanex with respect to the source point (4 m) to prevent low-energy electrons reaching the ICT coil.

Since then, a new generation of ICTs, turbo-ICTs, have been developed (Bergoz). Relying on the same physical principle as ICTs, they are coupled to a low-noise amplifier and an RF modulator which makes them optimized for low-charges (down to 10 fC) measurements. In addition, operated in the single-bunch mode, they can detect sub-nanosecond bunch charges of less than 1 pC. Turbo-ICTs have been implemented on an LPA for the first time on the COXINEL experiment (Labat *et al.*, 2014; Couprie *et al.*, 2016). One item was placed at the LPA source exit (*i.e.* inside the electron beam generation vacuum chamber) and another at the exit of the undulator. In both cases, a Lanex screen monitor was implemented just downstream of the turbo-ICT for bunch charge comparative measurements. As expected, the first turbo-ICT suffered from the strong EMP in the vicinity of the electron beam source and provided incoherent data. But the second one, 10 m downstream, gave charge measurements in very good agreement with the non-absolute-charge measurements (in CCD counts units) of the downstream Lanex screen. The correlation over 30 consecutive shots is illustrated in Fig. 2.

2.2. Spectrum measurements

2.2.1. Spectrum measurement techniques. On RFAs, electron beam spectrum measurements commonly rely on a dispersive element which spatially spans the beam on a detector. The same technique can be used on LPAs, provided that: (i) due to the very broad energy range expected, the detection area is large enough, and (ii) to deal with the high shot-to-shot fluctuations, the full spectrum can be acquired in one single shot. Variable magnetic fields in front of a fixed silicon detector were first used (Fritzler *et al.*, 2004; Malka *et al.*, 2001) but lacked the single-shot specification. Compact dipoles together with IPs (Tanaka *et al.*, 2005; Clayton *et al.*, 1995) were also tried but were limited in terms of repetition
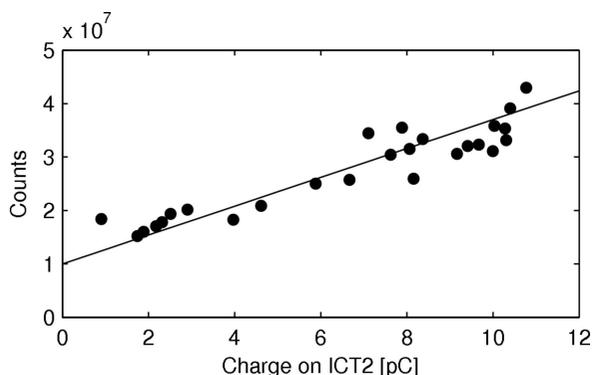
Figure 2
Charge measurements on the COXINEL experiment: number of counts recorded on the screen monitor IMG.5 within a 500 pixel diameter ROI *versus* charge measured on the turbo-ICT at the undulator exit. Black circles: measurements; full line: linear fit.

Figure 3
False color images of four unprocessed undulator radiation spectra [(*a*)–(*d*)] with corresponding electron spectra (correspondence indicated by white arrows). Respective values for the number of detected photons (after processing for toroidal mirror, grating and camera response), electron beam charge, and central energy are (*a*) 1.2×10^6, 0.9 pC and 92 MeV, (*b*) 7.7×10^6, 1.6 pC and 95 MeV, (*c*) 6.1×10^6, 2.0 pC and 108 MeV, and (*d*) 4.0×10^6, 1.3 pC and 122 MeV. From Anania *et al.* (2014).

rate. Finally, after scintillating fiber arrays (Sears *et al.*, 2010), scintillating screens appeared as the most adapted detector. Coupled to an appropriate imaging system, they enable single-shot full-range spectrum, charge and divergence measurement (Glinec *et al.*, 2006). A suitable choice of dipole strength, screen size and imaging magnification enables the desired resolution to be reached without fundamental limit.

2.2.2. Spectra on LPA-based SR experiments. In all LPA-based SR experiments (Schlenvoigt *et al.*, 2008; Fuchs *et al.*, 2009; Lambert *et al.*, 2012; Anania *et al.*, 2014; Couprie *et al.*, 2016) the electron beam spectrum was recorded using the following technique: electron beam imaging on a scintillator after passing through a dispersive (dipole) element. Even if the screen type [Konica TR (Schlenvoigt *et al.*, 2008), phosphor screen (Fuchs *et al.*, 2009), Lanex and Ce:YAG (Anania *et al.*, 2014; Couprie *et al.*, 2016)] or the dipole-type [permanent magnet (Schlenvoigt *et al.*, 2008; Fuchs *et al.*, 2009; Anania *et al.*, 2014) or electro-magnetic (Couprie *et al.*, 2016)] change from one setup to the other, all spectra are recorded in single shot and enable a broad-band energy distribution with a fluctuating mean value as well as spreading to be exhibited. An illustrative example is presented in the bottom half of Fig. 3.

2.3. Position measurements

2.3.1. Position measurement techniques. For an accurate alignment and focusing of the electron beam inside the undulator, mandatory for SR and further FEL light production, the electron beam position must be precisely measured. The standard instruments on RFAs (in particular LINACs) are striplines (Suwada *et al.*, 2000) and cavity beam-position monitors (cBPMs) (Hartman *et al.*, 1995; Keil *et al.*, 2010, 2013). Non-destructive and easily included into a feedback system, they provide a resolution that can reach the sub-micrometer level.

For LPAs, however, because of the large beam pointing (mrad) and shape fluctuations, the devices should allow a large detection area and be as insensitive as possible to the bunch profile. This is why, up to now, a scintillating screen imaged on
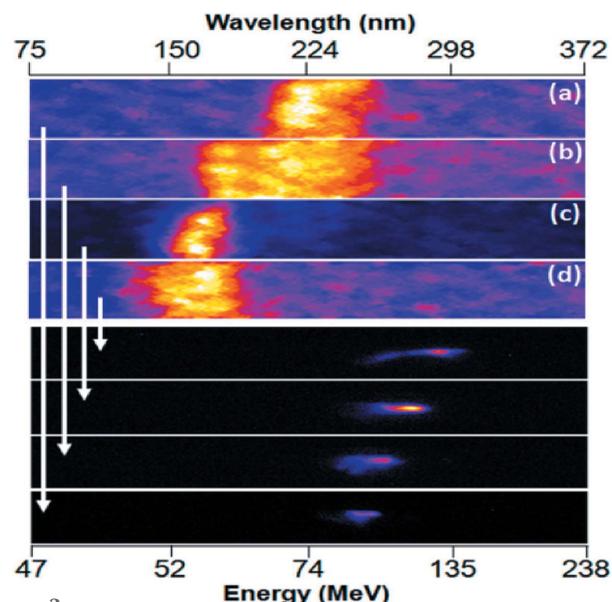
a CCD has been the preferred method. The final resolution can raise up to 500 µm and is hardly below the 10 µm level depending on the scintillator type (Tyrell, 2005), but most of the time it is enough due to the large divergence of the beams.

2.3.2. Position on LPA-based SR experiments. All LPA-based SR experiments used screen monitors for position measurements. They were first used for a rough observation of the beam position and shape, *i.e.* to check that the beam went more or less in and out of the undulator (Schlenvoigt *et al.*, 2008; Fuchs *et al.*, 2009; Lambert *et al.*, 2012). The first characterization of an LPA beam along a transport line was presented by Anania *et al.* (2014). Using four screen monitors distributed along the line, the beam shape evolution was observed and the beginning of a matching was attempted in the undulator. Still, there was no real control of the beam phase-space throughout the line. This was first achieved on COXINEL (Couprie *et al.*, 2018). Using six screen monitors, the beam could be observed: (i) at the LPA source exit, with or without the first triplet of quadrupoles to finally adjust the first stage of refocusing, (ii) in the middle of the chicane, with a non-zero dispersion, to measure the beam energy and energy spread, (iii) and (iv) at the undulator entrance and exit to finely tune the beam matching inside the undulator, and (vi) after the final dump dipole to remeasure the beam energy distribution at the end of the line. The beam manipulation mastering could essentially be performed thanks to the use of Ce:YAG screens instead of Lanex screens at the entrance and exit of the undulator (Labat *et al.*, 2014). In Fig. 4, a series of ten consecutive shots recorded on the screen monitor located at the undulator exit is presented. For the first five shots a
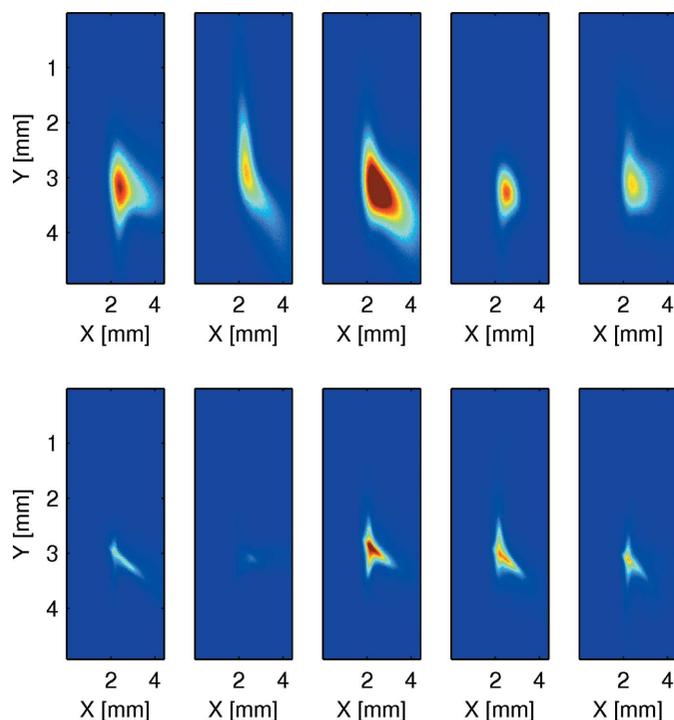
Figure 4
Consecutive beam profiles recorded at the undulator exit on the COXINEL experiment using (top) Lanex and (bottom) Ce:YAG screens. The color scale is fixed for all images.

Figure 5
Ce:YAG screen *versus* cBPM position measurement on the COXINEL (*a*) at the undulator entrance and (*b*) at the undulator exit. In both cases, the cBPM is just downstream of the screen monitor. (*a*) IMG.4 CCD *versus* cBPM1 measurements. (*b*) IMG.5 CCD *versus* cBPM2 measurements.

Lanex screen was used while for the last five shots a Ce:YAG screen was inserted (using a motorized stage to flip from one to the other). The Ce:YAG, owing to its lower thickness and smaller grain size, enables much more refined structures to be distinguished, although with a lower photon yield. Comparing the observed beam shape with the one expected from tracking simulations, we could finely optimize the transport down to the undulator.

The first installation of cBPMs on an LPA was also realised on COXINEL (Labat *et al.*, 2014; Couprie *et al.*, 2016), allowing the first on-line position measurements. A first item was placed at the undulator entrance and a second at the undulator exit, in both cases just upstream of a screen monitor for comparative measurements of the beam position. This comparison was achieved using a broad-band electron beam energy, *i.e.* spanning from 50 up to 220 MeV at the source point and from 150 to 190 MeV after spectral filtering in the chicane using an aluminium slit. As illustrated in Fig. 5, the agreement is still not very satisfactory. The discrepancy in the absolute amplitude of the beam displacements (obtained using steerers) can reach a factor of four and varies depending on the plane and the cBPM considered. Because of the large beam position fluctuations at the cBPM location (± 0.5 mm while a few tens of micrometers stability would have been required) and because of the low repetition rate (0.1 Hz or less), we could not achieve a proper calibration of the cBPMs. In addition, for a given machine setting, *i.e.* ideally fixed beam position, the cBPM gave position fluctuations far above those of t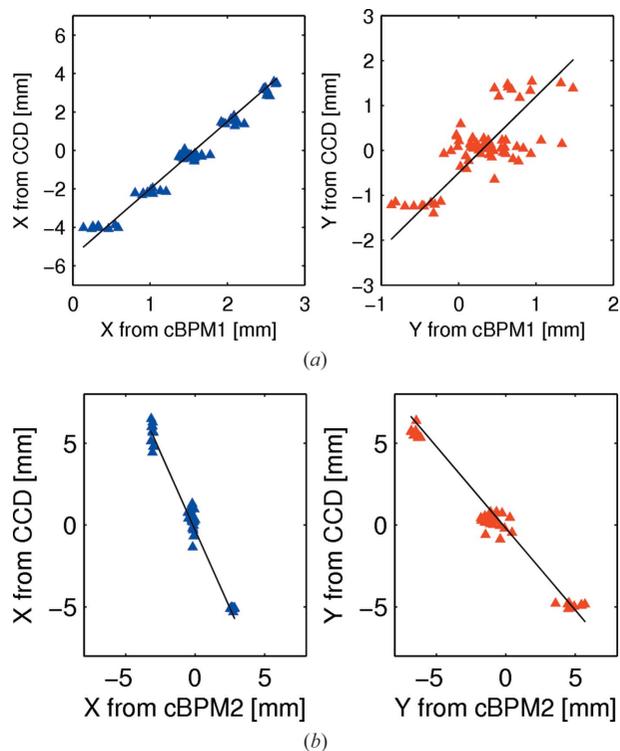he screen monitor and in an uncorrelated way. This is essentially due to the sensitivity of the cBPM to the bunch shape. cBPMs detect the center of mass of the particle distribution, while the screen monitor enables the center of the high density core beam, *i.e.* the part of interest, to be followed.

Nevertheless, the cBPMs provided an average position measurement in rather good relative agreement with the screen monitors, which is already one step towards on-line position measurements on LPAs. By filtering the beam in energy, we hope to improve the cBPMs' accuracy.

2.4. Bunch length measurements

2.4.1. Bunch length measurement techniques. Several techniques are in operation on RFAs. The streak camera (Lumpkin *et al.*, 1999) is easy to implement, but limited to picosecond resolutions. The transverse deflecting cavities (TDS) (Loew & Altenmueller, 1965; Behrens *et al.*, 2014) can be femtosecond-resolution but require implementation of an RF cavity which can be an issue in a non-RF environment as it is the case of most LPAs. On the other hand, coherent transition radiation (CTR) analysis (Wesch *et al.*, 2011; Maxwell *et al.*, 2013) and electro-optic sampling (EOS) (Yan *et al.*, 2000; Shan *et al.*, 2000; Wilke *et al.*, 2002), in their spectral or spatial encoding versions, enable single-shot and sub-picosecond resolution measurements. Because the LPA bunch length is typically of the order of the plasma wavelength, *i.e.* a few micrometers, femtosecond-resolution is required, and, again,

to cope with the large fluctuations, the measurement should be single shot. CTR and EOS were therefore naturally the methods implemented on LPAs (not yet on LPA-based SR experiments).

2.4.2. Bunch length measurements on LPAs. In 2006, the EOS technique in the temporal encoding version was used to measure bunch lengths of the order of 50 fs r.m.s. (Van Tilborg *et al.*, 2006). The CTR technique first enabled a sub-micrometer modulation of LPA beams at the laser wavelength in the laser plane of polarization, in good agreement with PIC simulations (Glinec *et al.*, 2007). A few years later, CTR was used to measure LPA bunch lengths of the order of 1.4–1.8 fs r.m.s. (Lundh *et al.*, 2011).

2.5. Emittance measurements

2.5.1. Emittance measurement techniques. The emittance is well known as the figure of merit for relativistic particles since it quantifies its divergence and focusability. But it is also a key parameter of the FEL gain and final brightness. Several methods have been proposed and implemented on RFAs to measure the geometric emittance. The quadrupole scan (Minty & Zimmermann, 2003) is a reliable thus not single-shot possibility. Using multiscreen image analysis at different betatron phases (Cutler *et al.*, 1987; Yakimenko *et al.*, 2002) is not single-shot and in addition requires a long and complicated transport, little suitable for LPAs. The multiple OTR screen analysis (Thomas *et al.*, 2011) was demonstrated to be a single-shot technique, though for GeV-range beam energies. Finally, the pepper-pot technique (Zhang, 1996; Yamazaki *et al.*, 1992), *i.e.* probing the phase-space with a mask of holes or slits, may be the only single-shot method for <GeV beams.

2.5.2. Emittance measurements on LPAs. The first two-dimensional and single-shot measurement using a pepper-pot on an LPA beam (Brunetti *et al.*, 2010) gave a normalized emittance of $\langle \varepsilon_{nx} \rangle = 2.2 \pm 0.7\pi$ mm mrad in the horizontal and $\langle \varepsilon_{nz} \rangle = 2.3 \pm 0.6\pi$ mm mrad in the vertical plane at 125 MeV (see Fig. 6). But a few years later, the limitations of this

Figure 7
The r.m.s. beam size *versus* beam energy for a single shot (circles). The solid fit line corresponds to a beam with normalized emittance of $0.14 \pm 0.01\pi$ mm mrad. The other lines show the expected functions for a 20% larger emittance by varying the inferred source size or divergence. From Weingartner *et al.* (2012).

technique in the case of LPA beams were clearly addressed (Cianchi *et al.*, 2013). LPA beams exhibit an ultra-thin phase-space due to their large divergence. The pepper-pot method proposes to sample this phase-space using holes or slits. Whatever the mask, the very low thickness of the phase-space may lead to an inefficient sampling resulting in large errors on the emittance estimate. In the case reported by Brunetti *et al.* (2010), this error might reach 47% assuming a 10 µm initial spot size and even 1000% assuming a 1 µm initial spot size. The quadrupole scan method, on the other hand, in spite of being single-shot, might only be limited by the beam size inside the quadrupoles. Provided this size is small enough to avoid chromatic effects and consequent emittance dilution, the method should remain reliable in the case of LPAs. This method was actually implemented with success to measure sub-mm mrad emittance as reported by Weingartner *et al.* (2012). In the same publication, an alternative single-shot method was also proposed and demonstrated: the energy scan. Using two quadrupoles to focus the beam in the horizontal plane and one dipole to disperse the beam in energy in the vertical plane, a two-dimensional beam distribution can be recorded on a scintillator. Further, fitting the horizontal beam size as a function of the beam energy provides the geometric emittance in one single-shot (see Fig. 7). Both methods, quadrupole and energy scan, were found to be in 10% agreement. Finally, it is also possible to estimate an LPA beam emittance using spectroscopy (Plateau *et al.*, 2012): it is a single-shot thus indirect measurement.

3. Photon diagnostics

3.1. Background issues

Prior to the implementation of photon diagnostics, background issues should be addressed. Indeed, LPAs suffer from a very 'high light' environment resulting from at least three type of sources. The IR laser which is used for electron beam generation is tightly focused at the source point and therefore
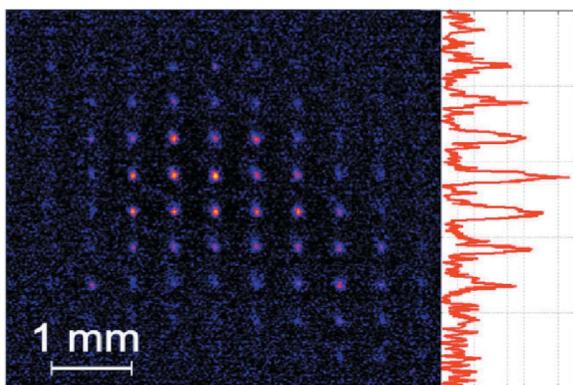

Figure 6
False-color background-corrected pepper-pot image produced on the Ce:YAG crystal by an electron beam after propagation through the emittance mask. A vertical lineout is shown on the right-hand side. Reprinted with permission from Brunetti *et al.* (2010), *Phys. Rev. Lett.* **105**, 215007. Copyright (2010) by the American Physical Society.
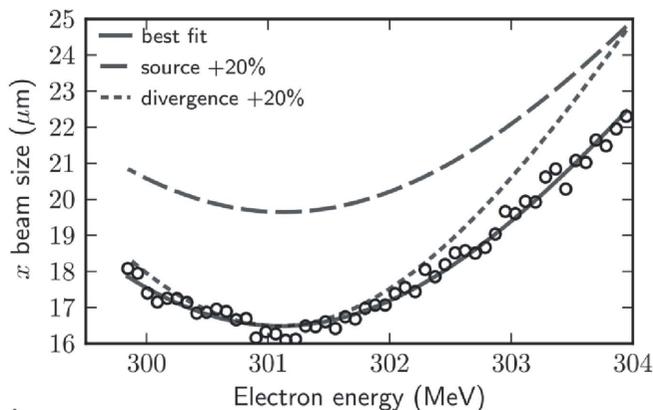
very divergent downstream. Nevertheless, because it is also ultra-intense and unfortunately well guided by metallic vacuum pipes, the laser intensity remains nothing but negligible even meters downstream. In all LPA-based SR experiments, aluminium foils on the laser path were used to cut this IR laser. But, though not estimated in the corresponding publications, the effect of those foils can be dramatic on the slice emittance. Applying simple analytical formulae (Chao & Tigner, 1999) to a typical LPA beam (100 MeV, 1π mm mrad slice emittance) with a magnification of 1/20 in the undulator, we found that an aluminium foil on the beam path would multiply the slice emittance by a factor of ten for a thickness of 15 μm as used by Schlenvoigt *et al.* (2008) and Fuchs *et al.* (2009) and by a factor of two for a thickness of 500 nm as more or less used by Anania *et al.* (2014) and Couprie *et al.* (2018). The only alternative, to our knowledge, would be the use of a dogleg, but this would lead to other issues of transport.

The plasma created by the intense IR laser also produces a strong isotropic illumination in the visible range, together with a wide range of particles (X-rays, gamma-rays, *etc.*). This parasitic 'light' can easily reach all the detection system implemented in the accelerator room and requires all the diagnostics, and in particular photon diagnostics, to be carefully protected using bandpass filters, blockers, shielding, *etc.*

In addition to these comes the coherent and incoherent radiation which is systematically emitted when the electron beam crosses the plasma–vacuum transition at the source exit and the metallic foil previously mentioned. This component may often be negligible with respect to the previous ones, but should still be addressed.

3.2. Spectrum measurements

The present LPA-based SR experiments and near-future LPA-based FEL experiments do not have to deal with users and can afford a destructive spectrum measurement. Therefore, basic spectrometers relying on a grating and a CCD were simply implemented, eventually coupled to collecting optics. Because the initial LPA beam highly fluctuates in energy, the resulting SR spectra are also expected to fluctuate, requiring single-shot measurements and simultaneous recording of the electron beam spectral content. The most illustrative example of LPA-based SR spectrum measurement is presented in Fig. 3. It first shows that this kind of spectrometer (grating with CCD) enables the measurement of both the beam energy content (along the horizontal axis) and divergence (along the vertical axis). It also shows that the central SR wavelength can fluctuate by more than 25% because of the initial beam energy variations.

3.3. Beam profile measurements

Like on synchrotron beamlines or FEL beamlines, the radiation profile can be measured directly using a CCD or indirectly using an intermediate scintillator.

The first beam profile measurement of LPA-based SR was reported by Lambert *et al.* (2012) and is shown in Fig. 8. The footprint was recorded without any spectral filtering, *i.e.* in a
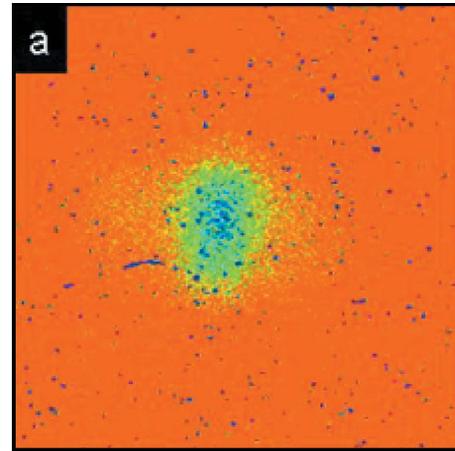
Figure 8
Single-shot footprint of the radiation measured on the CCD camera. From Lambert *et al.* (2012).

wide (230–440 nm) range, and the *SRW* (Chubar & Elleaume, 1998) simulations only matched in one plane, probably because of remaining parasitic light in the horizontal direction. Beam-profile systematic measurements were recently achieved on COXINEL, but their analysis is still on-going.

4. Conclusion

Diagnostics for LPA beams and LPA-based SR are not yet satisfactory. But LPA is a much more recent technology which still needs time to adapt or develop its diagnostics. The basic tools already exist for a full characterization of an LPA beam along a complex transport line, and for the analysis of consequent SR or FEL radiation. But both beam characterization and further FEL applications would highly benefit further improvement of on-line diagnostics to survey the LPA stage.

The demonstration of an LPA-based FEL is still to be achieved but, thanks to advanced ideas of beam manipulation, this no longer stands in the distant future.

References

Ackermann, W. *et al.* (2007). *Nat. Photon.* **1**, 336–342.
Allaria, E., Castronovo, D., Cinquegrana, P., Craievich, P., Dal Forno, M., Danailov, M. B., D'Auria, G., Demidovich, A., De Ninno, G., Di Mitri, S., Diviacco, B., Fawley, W. M., Ferianis, M., Ferrari, E., Froehlich, L., Gaio, G., Gauthier, D., Giannessi, L., Ivanov, R., Mahieu, B., Mahne, N., Nikolov, I., Parmigiani, F., Penco, G., Raimondi, L., Scafuri, C., Serpico, C., Sigalotti, P., Spampinati, S.,

Spezzani, C., Svandrlik, M., Svetina, C., Trovo, M., Veronese, M., Zangrando, D. & Zangrando, M. (2013). *Nat. Photon.* **7**, 913–918.

Anania, M. P., Brunetti, E., Wiggins, S. M., Grant, D. W., Welsh, G. H., Issac, R. C., Cipiccia, S., Shanks, R. P., Manahan, G. G., Aniculaesei, C., van der Geer, S. B., de Loos, M. J., Poole, M. W., Shepherd, B. J. A., Clarke, J. A., Gillespie, W. A., MacLeod, A. M. & Jaroszynski, D. A. (2014). *Appl. Phys. Lett.* **104**, 264102.

Behrens, C., Decker, F.-J., Ding, Y., Dolgashev, V. A., Frisch, J., Huang, Z., Krejcik, P., Loos, H., Lutman, A., Maxwell, T. J., Turner, J., Wang, J., Wang, M.-H., Welch, J. & Wu, J. (2014). *Nat. Commun.* **5**, 4762.

Brown, K. L. & Tautfest, G. W. (1956). *Rev. Sci. Instrum.* **27**, 696.

Brunetti, E., Shanks, R. P., Manahan, G. G., Islam, M. R., Ersfeld, B., Anania, M. P., Cipiccia, S., Issac, R. C., Raj, G., Vieux, G., Welsh, G. H., Wiggins, S. M. & Jaroszynski, D. A. (2010). *Phys. Rev. Lett.* **105**, 215007.

Chao, A. & Tigner, M. (1999). *Handbook of Accelerator Physics and Engineering*, p. 267. Singapore: World Scientfic.

Chien, T. Y., Chang, C. L., Lee, C. H., Lin, J. Y., Wang, J. & Chen, S. Y. (2005). *Phys. Rev. Lett.* **94**, 115003.

Chubar, O. & Elleaume, P. (1998). *Proceedings of the Sixth European Particle Accelerator Conference (EPAC'98)*, Stockholm, Sweden, pp. 1177–1179.

Cianchi, A., Anania, M. P., Bellaveglia, M., Castellano, M., Chiadroni, E., Ferrario, M., Gatti, G., Marchetti, B., Mostacci, A., Pompili, R., Ronsivalle, C., Rossi, A. R. & Serafini, L. (2013). *Nucl. Instrum. Methods Phys. Res. A*, **720**, 153–156.

Clayton, C. *et al.* (1995). *Proceedings of the 1995 Particle Accelerator Conference and International Conference on High Energy Accelerators*, 1–5 May 1995, Dallas, TX, USA. Unpublished.

Couprie, M. E. *et al.* (2018) Submitted.

Couprie, M. E., Labat, M., Evain, C., Marteau, F., Briquez, F., Khojoyan, M., Benabderrahmane, C., Chapuis, L., Hubert, N., Bourassin-Bouchet, C., El Ajjouri, M., Bouvet, F., Dietrich, Y., Valléau, M., Sharma, G., Yang, W., Marcouillé, O., Vétéran, J., Berteaud, P., El Ajjouri, T., Cassinari, L., Thaury, C., Lambert, G., Andriyash, I., Malka, V., Davoine, X., Tordeux, M. A., Miron, C., Zerbib, D., Tavakoli, K., Marlats, J. L., Tilmont, M., Rommeluère, P., Duval, J. P., N'Guyen, M. H., Rouqier, A., Vanderbergue, M., Herbeaux, C., Sebdouai, M., Lestrade, A., Leclercq, N., Dennetière, D., Thomasset, M., Polack, F., Bielawski, S., Szwaj, C. & Loulergue, A. (2016). *Plasma Phys. Contrib. Fusion*, **58**, 034020.

Couprie, M. E., Loulergue, A., Labat, M., Lehe, R. & Malka, V. (2014). *J. Phys. B*, **47**, 234001.

Cutler, R. I., Owen, J. & Whittaker, J. (1987). *Proceedings of the 1987 IEEE Particle Accelerator Conference (PAC'87)*, 16–19 March 1987, Washington, DC, USA. p. 625.

Dattoli, G., Giannessi, L., Renieri, A. & Torre, A. (1993). *Prog. Opt.* **31**, 321.

Emma, P., Akre, R., Arthur, J., Bionta, R., Bostedt, C., Bozek, J., Brachmann, A., Bucksbaum, P., Coffee, R., Decker, F.-J., Ding, Y., Dowell, D., Edstrom, S., Fisher, A., Frisch, J., Gilevich, S., Hastings, J., Hays, G., Hering, P., Huang, Z., Iverson, R., Loos, H., Messerschmidt, M., Miahnahri, A., Moeller, S., Nuhn, H.-D., Pile, G., Ratner, D., Rzepiela, J., Schultz, D., Smith, T., Stefan, P., Tompkins, H., Turner, J., Welch, J., White, W., Wu, J., Yocky, G. & Galayda, J. (2010). *Nat. Photon.* **4**, 641–647.

Faure, J., Glinec, Y., Pukhov, A., Kiselev, S., Gordienko, S., Lefebvre, E., Rousseau, J. P., Burgy, F. & Malka, V. (2004). *Nature (London)*, **431**, 541–544.

Faure, J., Rechatin, C., Norlin, A., Lifschitz, A., Glinec, Y. & Malka, V. (2006). *Nature (London)*, **444**, 737–739.

Fritzler, S., Lefebvre, E., Malka, V., Burgy, F., Dangor, A. E., Krushelnick, K., Mangles, S. P. D., Najmudin, Z., Rousseau, J.-P. & Walton, B. (2004). *Phys. Rev. Lett.* **92**, 165006.

Fuchs, M., Weingartner, R., Popp, A., Major, Z., Becker, S., Osterhoff, J., Cortrie, I., Zeitler, B., Hörlein, R., Tsakiris, G. D., Schramm, U.,

Rowlands-Rees, T. P., Hooker, S. M., Habs, D., Krausz, F., Karsch, S. & Grüner, F. (2009). *Nat. Phys.* **5**, 826–829.

Geddes, C. G. R., Nakamura, K., Plateau, G. R., Toth, C., Cormier-Michel, E., Esarey, E., Schroeder, C. B., Cary, J. R. & Leemans, W. P. (2008). *Phys. Rev. Lett.* **100**, 215004.

Geddes, C. G., Toth, C. S., Van Tilborg, J., Esarey, E., Schroeder, C. B., Bruhwiler, D., Nieter, C., Cary, J. & Leemans, W. P. (2004). *Nature (London)*, **431**, 538–541.

Glinec, Y., Faure, J., Guemnie-Tafo, A., Malka, V., Monard, H., Larbre, J. P., De Waele, V., Marignier, J. L. & Mostafavi, M. (2006). *Rev. Sci. Instrum.* **77**, 103301.

Glinec, Y., Faure, J., Norlin, A., Pukhov, A. & Malka, V. (2007). *Phys. Rev. Lett.* **98**, 194801.

Hartman, S. C., Shintake, T. & Akasaka, N. (1995). *Nanometer Resolution BPM using Damped-Slot Resonator.* Report SLAC-PUB-95-6908. SLAC, Stanford, CA 94309, USA.

Huang, Z., Ding, Y. & Schroeder, C. B. (2012). *Phys. Rev. Lett.* **109**, 204801.

Ishikawa, T. *et al.* (2012). *Nat. Photon.* **6**, 540–544.

Keil, B., Baldinger, R., Ditter, R., Koprek, W., Kramert, R., Marcellini, F., Marinkovic, G., Roggli, M., Rohrer, M., Stadler, M., & Treyer, D. M. (2013). *Proceedings of the 2nd International Beam Instrumentation Conference (IBIC2013)*, 16–19 September 2013, Oxford, UK, p. 427.

Keil, B., Baldinger, R., Ditter, R., Kramert, R., Marinkovic, G., Pollet, P., Roggli, M., Rohrer, M., Schlott, V., Stadler, M., Treyer, D. M., Decking, W., Lipka, D., Nölle, D., Siemens, M., Traber, T., Vilcins, S., Napoly, O., Simon, C. S., Prestel, J.-P. & Rouvière, N. (2010). *Proceedings of the First International Particle Accelerator Conference (IPAC'10)*, Kyoto, Japan, p. 1125.

Kim, K. J. & Xie, M. (1993). *Nucl. Instrum. Methods Phys. Res. A*, **331**, 359–364.

Labat, M., Cassinari, L., Couprie, M. E., El Ajjouri, M.-E., Hubert, N. & Loulergue A. (2014). *Proceedings of the FEL'2014 Conference*, 25–29 August 2014, Basel, Switzerland, pp. 937–940.

Lambert, G., Corde, S., Ta phuoc, K., Malka, V., Ben Ismail, A., Benveniste, E., Specka, A., Labat, M., Loulergue, A., Briquez, F. & Couprie, M. E. (2012). *Proceedings of the 34th International Free-Electron Laser Conference (FEL2012)*, 26–31 August 2012, Nara, Japan. JACoW.

Leemans, W. P., Nagler, B., Gonsalves, A. J., Tóth, C., Nakamura, K., Geddes, C. G. R., Esarey, E., Schroeder, C. B. & Hooker, S. M. (2006). *Nat. Phys.* **2**, 696–699.

Loew, G. A. & Altenmueller, O. H. (1965). *Proceedings of the Fifth International Conference on High-Energy Accelerators*, Frascati, Italy, 9–16 September 1965. SLAC-PUB-135.

Loulergue, A., Labat, M., Evain, C., Benabderrahmane, C., Malka, V. & Couprie, M. E. (2015). *New J. Phys.* **17**, 023028.

Lumpkin, A. H., Yang, B. X., Berg, W. J., White, M., Lewellen, J. W. & Milton, S. V. (1999). *Nucl. Instrum. Methods Phys. Res. A*, **429**, 336–340.

Lundh, O., Lim, J., Rechatin, C., Ammoura, L., Ben-Ismaïl, A., Davoine, X., Gallot, G., Goddet, J.-P., Lefebvre, E., Malka, V. & Faure, J. (2011). *Nat. Phys.* **7**, 219–222.

Madey, J. M. J. (1971). *J. Appl. Phys.* **42**, 1906–1913.

Maier, A. R., Meseck, A., Reiche, S., Schroeder, C. B., Seggebrock, T. & Grüner, F. (2012). *Phys. Rev. X*, **2**, 031019.

Malka, V., Faure, J., Marquès, J. R., Amiranoff, F., Rousseau, J. P., Ranc, S., Chambaret, J. P., Najmudin, Z., Walton, B., Mora, P. & Solodov, A. (2001). *Phys. Plasmas*, **8**, 2605–2608.

Mangles, S. P. D., Murphy, C. D., Najmudin, Z., Thomas, A. G. R., Collier, J. L., Dangor, A. E., Divall, E. J., Foster, P. S., Gallacher, J. G., Hooker, C. J., Jaroszynski, D. A., Langley, A. J., Mori, W. B., Norreys, P. A., Tsung, F. S., Viskup, R., Walton, B. R. & Krushelnick, K. (2004). *Nature (London)*, **431**, 535–538.

Maxwell, T. J., Behrens, C., Ding, Y., Fisher, A. S., Frisch, J., Huang, Z. & Loos, H. (2013). *Phys. Rev. Lett.* **111**, 184801.

Minty, M. G. & Zimmermann, F. (2003). *Measurement and Control of Charged Particle Beams.* New York: Springer.

Nakamura, K., Gonsalves, A. J., Lin, C., Smith, A., Rodgers, D., Donahue, R., Byrne, W. & Leemans, W. P. (2011). *Phys. Rev. ST Accel. Beams*, **14**, 062801.

Pittman, M., Ferré, S., Rousseau, J. P., Notebaert, L., Chambaret, J. P. & Chériaux, G. (2002). *Appl. Phys. B*, **74**, 529–535.

Plateau, G. R., Geddes, C. G. R., Thorn, D. B., Chen, M., Benedetti, C., Esarey, E., Gonsalves, A. J., Matlis, N. H., Nakamura, K., Schroeder, C. B., Shiraishi, S., Sokollik, T., van Tilborg, J., Toth, C., Trotsenko, S., Kim, T. S., Battaglia, M., Stöhlker, Th. & Leemans, W. P. (2012). *Phys. Rev. Lett.* **109**, 064802.

Pukhov, A. & Meyer-ter-Vehn, J. (2002). *Appl. Phys. B*, **74**, 355–361.

Rogowski, W. & Steinhaus, W. (1912). *Arch. Elektrotech.* **1**, 141150.

Schlenvoigt, H.-P., Haupt, K., Debus, A., Budde, F., Jäckel, O., Pfotenhauer, S., Schwoerer, H., Rohwer, E., Gallacher, J. G., Brunetti, E., Shanks, R. P., Wiggins, S. M. & Jaroszynski, D. A. (2008). *Nat. Phys.* **4**, 130–133.

Schroeder, C. B. *et al.* (2012). *ICFA Workshop on Future Light Sources (FLS2012)*, 5–9 March 2012, Newport News, VA, USA. Unpublished.

Sears, C. M. S., Cuevas, S. B., Schramm, U., Schmid, K., Buck, A., Habs, D., Krausz, F. & Veisz, L. (2010). *Rev. Sci. Instrum.* **81**, 073304.

Seggebrock, T., Maier, A. R., Dornmair, I. & Grüner, F. (2013). *Phys. Rev. ST Accel. Beams*, **16**, 070703.

Shan, J., Weling, A. S., Knoesel, E., Bartels, L., Bonn, M., Nahata, A., Reider, G. A. & Heinz, T. F. (2000). *Opt. Lett.* **25**, 426–428.

Suwada, T., Kamikubota, N., Fukuma, H., Akasaka, N. & Kobayashi, H. (2000). *Nucl. Instrum. Methods Phys. Res. A*, **440**, 307–319.

Tajima, T. & Dawson, J. M. (1979). *Phys. Rev. Lett.* **43**, 267–270.

Tanaka, K. A., Yabuuchi, T., Sato, T., Kodama, R., Kitagawa, Y., Takahashi, T., Ikeda, T., Honda, Y. & Okuda, S. (2005). *Rev. Sci. Instrum.* **76**, 013507.

Thomas, C., Delerue, N. & Bartolini, R. (2011). *J. Instrum.* **6**, P07004.

Tyrell, G. C. (2005). *Nucl. Instrum. Methods Phys. Res. A*, **546**, 180–187.

Unser, K. B. *et al.* (1989). *Proceedings of the 1989 Particle Accelerator Conference*, Chicago, IL, USA, 20–23 March 1989, Vol. 1, p. 71.

Van Tilborg, J., Schroeder, C. B., Filip, C. V., Tóth, Cs., Geddes, C. G. R., Fubiani, G., Huber, R. A., Kaindl, R., Esarey, E. & Leemans, W. P. (2006). *Phys. Rev. Lett.* **96**, 014801.

Weingartner, R., Raith, S., Popp, A., Chou, S., Wenz, J., Khrennikov, K., Heigoldt, M., Maier, A. R., Kajumba, N., Fuchs, M., Zeitler, B., Krausz, F., Karsch, S. & Grüner, F. (2012). *Phys. Rev. ST Accel. Beams* **15**, 111302.

Wesch, S., Schmidt, B., Behrens, C., Delsim-Hashemi, H. & Schmüser, P. (2011). *Nucl. Instrum. Methods Phys. Res. A*, **665**, 40–47.

Wilke, I., MacLeod, A. M., Gillespie, W. A., Berden, G., Knippels, G. M. H. & van der Meer, A. F. G. (2002). *Phys. Rev. Lett.* **88**, 124801.

Yakimenko, V., Babzien, M., Ben-Zvi, I., Malone, R. & Wang, X. (2002). *Nucl. Instrum. Methods Phys. Res. A*, **483**, 277–281.

Yamazaki, Y., Kurihara, T., Kobayashi, H., Sato, I. & Asami, A. (1992). *Nucl. Instrum. Methods Phys. Res. A*, **322**, 139–145.

Yan, X., MacLeod, A. M., Gillespie, W. A., Knippels, G. M. H., Oepts, D., van der Meer, A. F. G. & Seidel, W. (2000). *Phys. Rev. Lett.* **85**, 3404–3407.

Zeil, K., Kraft, S. D., Jochmann, A., Kroll, F., Jahr, W., Schramm, U., Karsch, L., Pawelke, J., Hidding, B. & Pretzler, G. (2010). *Rev. Sci. Instrum.* **81**, 013307.

Zewail, A. (2003). *Nobel Lectures in Chemistry 1996–2000*, edited by Ingmar Grenthe, *Nobel 47 Lecture of 1999.* Singapore: World Scientific.

Zhang, M. (1996). *Emittance Formula for Slits and Pepper-pot Measurement*, Report FERMILAB-TM-1998. Fermi National Accelerator Laboratory, Batavia, IL, USA.